Image to physical space registration of supine breast MRI for image guided breast surgery

Rebekah H. Conley[a], Ingrid M. Meszoely[b] ,Thomas S. Pheiffer[a], Jared A. Weis [c], Thomas E. Yankeelov[a,c,d,e], Michael I. Miga[a,e,f]

[a]Vanderbilt University Department of Biomedical Engineering, [b]Vanderbilt University Medical Center, Vanderbilt-Ingram Cancer Center, Division of Surgical Oncology, [c]Vanderbilt University Institute of Imaging Science, [d]Vanderbilt University Department of Physics and Astronomy, [e]Vanderbilt University Medical Center, Department of Radiology and Radiological Sciences, [f]Vanderbilt University Medical Center Department of Neurological Surgery, Nashville TN, USA

ABSTRACT

Breast conservation therapy (BCT) is a desirable option for many women diagnosed with early stage breast cancer and involves a lumpectomy followed by radiotherapy. However, approximately 50% of eligible women will elect for mastectomy over BCT despite equal survival benefit (provided margins of excised tissue are cancer free) due to uncertainty in outcome with regards to complete excision of cancerous cells, risk of local recurrence, and cosmesis. Determining surgical margins intraoperatively is difficult and achieving negative margins is not as robust as it needs to be, resulting in high re-operation rates and often mastectomy. Magnetic resonance images (MRI) can provide detailed information about tumor margin extents, however diagnostic images are acquired in a fundamentally different patient presentation than that used in surgery. Therefore, the high quality diagnostic MRIs taken in the prone position with pendant breast are not optimal for use in surgical planning/guidance due to the drastic shape change between preoperative images and the common supine surgical position. This work proposes to investigate the value of supine MRI in an effort to localize tumors intraoperatively using image-guidance. Mock intraoperative setups (realistic patient positioning in non-sterile environment) and preoperative imaging data were collected from a patient scheduled for a lumpectomy. The mock intraoperative data included a tracked laser range scan of the patient's breast surface, tracked center points of MR visible fiducials on the patient's breast, and tracked B-mode ultrasound and strain images. The preoperative data included a supine MRI with visible fiducial markers. Fiducial markers localized in the MRI were rigidly registered to their mock intraoperative counterparts using an optically tracked stylus. The root mean square (RMS) fiducial registration error using the tracked markers was 3.4mm. Following registration, the average closest point distance between the MR generated surface nodes and the LRS point cloud was 1.76±0.502 mm.

Keywords: breast cancer, lumpectomy, surgical guidance, registration, ultrasound, MRI, BCT

1. INTRODUCTION

Due to mass breast cancer screenings, women are being diagnosed at earlier stages with smaller tumors. Therefore, breast conserving therapy (BCT) is a viable option for many women with early stage breast cancer, provided that negative margins (no cancer cells present on resected specimen) and acceptable cosmetic outcomes can be achieved. Breast conserving therapy involves a lumpectomy (removal of tumor with a margin of surrounding healthy tissue) followed by radiation therapy. For decades, BCT has shown to have the same survival rate as mastectomy (removal of the whole breast) [1-3] in properly selected patients. However, there is an increasing trend toward choosing mastectomy over BCT due to surgical uncertainties [4], despite recent research showing BCT to have improved disease-specific survival over mastectomy [5].

The hesitation to choose BCT over mastectomy derives from the fact that determining surgical tumor margins intraoperatively is very difficult and negative margins are not always achieved, resulting in the need for a second surgery or mastectomy. Positive margins are often a result of an inability to visualize tumor location. Current techniques to localize breast lesions in the operating room include wire-guide localization and intraoperative ultrasound. Intraoperative ultrasound guidance is often ineffective for non-palpable breast tumors as approximately only half of these tumors can be visualized with ultrasonography [6]. The standard technique for intraoperative tumor localization is

wire-guided localization in which a radiologist inserts a wire into the tumor with guidance of ultrasound or mammography prior to entering the operating room. The surgeon then resects through the tissue being directed by the wire trajectory to the breast lesion. The shortcomings of this approach is that the guide wire does not provide a 3D perspective of the tumor and therefore cannot delineate tumor boundaries, which contributes to an unacceptable high rate of positive margins [7]. In addition, often the trajectory of the wire is dictated by the mammographic guidance and can at times represent an inefficient surgical route to the target which would direct the surgeon to navigate through excessive amounts of tissue, or would require the surgeon to make an visual estimation of a better route, both potentially leading to navigational errors.

Magnetic resonance (MR) imaging is the preferred imaging modality for preoperative clinical assessment and planning [7]. However, preoperative planning images are acquired in the prone position with breast pendant, while surgery is performed in the supine position with arm extended. The breast undergoes significant deformation and shape change between the two positions. While prone breast MR images have superior image quality, they are not particularly valuable for surgical planning. Prone to supine image registration of breast MRI for aid in surgical planning has previously been proposed [8-11]. Alternatively, in the work presented here, we propose to register supine MR images to physical space for intraoperative tumor localization. This approach has clear advantages: (1) the breast anatomy within the image volume is in a presentation that is representative of the operative setting, (2) tumor volume changes as it deforms under the breast's weight are captured better and should reflect better correlation between pathology reports and intraoperative observations, and (3) image-to-physical registration methods will be facilitated more readily.

Mock intraoperative data and preoperative data were collected from a patient scheduled for lumpectomy. The mock intraoperative data represents the localization of the patient's breast in physical space via multiple digitization methods (optically tracked laser range scan, stylus, and ultrasound imaging). Preoperative data includes MR images of the breast containing the lesion acquired in the supine orientation with MR-visible markers attached. Image to physical space registration was performed using landmarks visible in both the MR images and in physical space. The fiducial registration error (FRE), a measure of overall landmark misalignment, is reported as well as the closest point distance maps and average.

2. METHODS

Preoperative data collection and patient specific modeling

In the imaging phase of the experiments, adhesive MR visible fiducial markers (IZI Medical Products, Owing Mills, MD) were distributed across the surface of the breast prior to imaging. The patient was placed in the supine position with some elevation provided underneath the patient to position the breast as close to intraoperative orientation as possible within a closed bore 3T Philips scanner. T1-weighted, 3D turbo field echo (TFE) with fat suppression images were acquired using a cardiac coil carefully placed as to not deform the breast surface. The acquired image volume was 512 x 512 x 160 with a reconstructed voxel size of 0.391x0.391x1-mm .

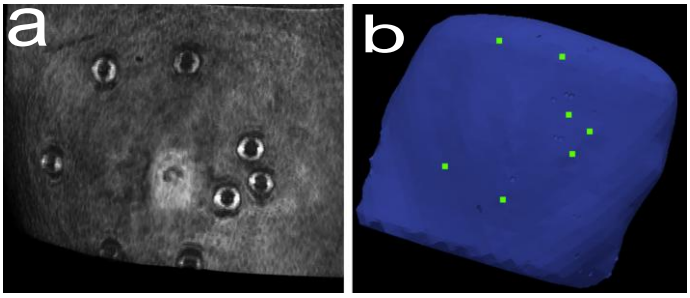

Figure 1 : A) Volume render of supine breast MRI. B) Patient specific finite element mesh. Green points are manually selected fiducial centers.

The breast and pectoral muscle was segmented using a semi-automatic active contour technique by ITK-SNAP's [12] implementation of the Snakes [13] algorithm. The tumor was manually segmented and exported as a mesh from ITK-SNAP. A standard marching cubes algorithm [14] was used to create an isosurface of the breast and pectoral muscle and was further smoothed using FastRBF Toolbox (Farfield Technologies, Christchurch, New Zealand). From this surface, a tetrahedral mesh was generated using a custom mesh generator [15]. A volume render of the breast surface and the mesh

generated by the MR volume is shown in Figure 1a. The green points in Figure 1B indicate the centers of the markers and were manually determined using Analyze 9.0 (Mayo Clinic, Rochester, MN, USA).

Mock intraoperative data collection

In our mock intraoperative setup, the patient was placed in a typical surgical orientation by a surgical oncologist to accurately depict operating room positioning. An optically tracked laser range scanner was used to scan the breast surface, providing a textured point cloud of the breast surface with known 3D coordinates. An optically tracked pen probe was used to collect the location of the centers of each of the fiducial markers. Finally, tracked ultrasound images were collected to provide the physical location of the tumor with respect to the breast surface. In this experiment ultrasound images were acquired using the Acuson Antares system (Siemens Medical Solutions USA, inc, Mountain View, CA) using a VFX13-5 linear array probe with the a depth of 6cm and frequency of 10 MHz. The ultrasound images were tracked in 3D by collecting synchronized video and tracking data on a host PC with the utilization of software based on the Visualization Toolkit (VTK). The ultrasound images were calibrated to physical space using a method [16] based on the relationship between an optically tracked pointer and an optically tacked ultrasound transducer. Image to physical space registration between points located in the ultrasound image plane and their physical space counterparts determined by the tracked pen probe was used to transform an ultrasound image into physical space. Following calibration, the compression of tissue caused by the ultrasound transducer was compensated for using a model based correction technique [18].

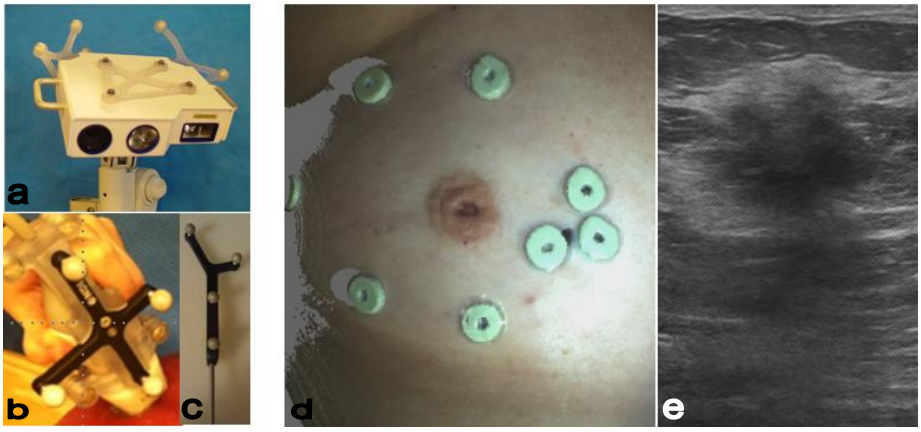

Figure 2: A) Laser range scanner with rigid bodies for tracking. B) Ultrasound transducer with rigid body for tracking. C) Tracked pen probe. D) Textured point cloud produced by tracked laser range scanner with known 3D coordinates. The green rings are MR visible adhesive fiducial markers. The centers of these markers are used for fiducials in registration. E) Example of a 2D ultrasound slice of the tumor (dark shadow shown by red arrow).

Registration technique

MR-digitized marker locations were rigidly registered to the mock intraoperative tracked stylus points using a 3D point-based singular value decomposition registration algorithm [17], yielding a 4x4 transformation matrix. The fiducial registration error (FRE), a measure of overall landmark misalignment, is reported according to equation 1. The transformed points are represented by $T(x_i)$, N is the number of points, and y_i is the corresponding point that $T(x_i)$ is aligned with by the transformation.

$$FRE = \sqrt{\frac{1}{N}\sum_i^N (T(x_i) - y_i)^2} \quad (1)$$

With respect to surface fit assessment, the closest point distance map between the LRS point cloud and the MR generated mesh is reported.

Subsurface validation and ultrasound image processing

Compression of the breast tissue by the ultrasound transducer leads to incorrect measurements of tumor size and location. In this paper, we utilize a previously developed model based correction scheme developed by Phieffer et al [18] to compensate for the compression of the target by the ultrasound transducer. The method utilizes the position of the tracked ultrasound probe to measure 3D displacements to drive a linear elastic correction model. The relative positions

of the probe surface can be used to estimate the displacement of the breast tissue. Once a registration is made between the patient specific MR mesh and physical space, the ultrasound probe is now in the same space as the mesh. The probe surface will be located slightly below the surface of the mesh, depending on the compression of the tissue by the user. The pose of the probe surface provides Dirichlet boundary conditions for a forward linear elastic model that deforms the patient specific mesh to the compressed state exerted by the probe. The deformation field generated by this model is then applied in reverse manner to deform/correct the ultrasound slices and the segmented tumor contours such that they are correctly rendered in the uncompressed state associated with the pre-procedural supine MR orientation.

The subsurface tumor registration accuracy was measured by comparing the location of the tumor contour in the *compression corrected* ultrasound image and the tumor contour in the MR volume. The distance between the centroid of the US tumor and the MR tumor is reported. The modified Hausdorff distance (MHD) [19] between the MR tumor contour and the US image contour is reported for seven ultrasound slices. The MHD is defined for two contours, A and B in accordance with equations 2 and 3. The mean closest point distance d(A,B) is calculated in the direction from A to B, and then again from B to A. MHD is the maximum mean closest point between the two contours.

$$d(A,B) = \frac{1}{N_a}\sum_{a\epsilon A} min_{b\epsilon B}(||a-b||) \quad (2)$$

$$MHD = \max\left(d(A,B), d(B,A)\right) \quad (3)$$

3. RESULTS

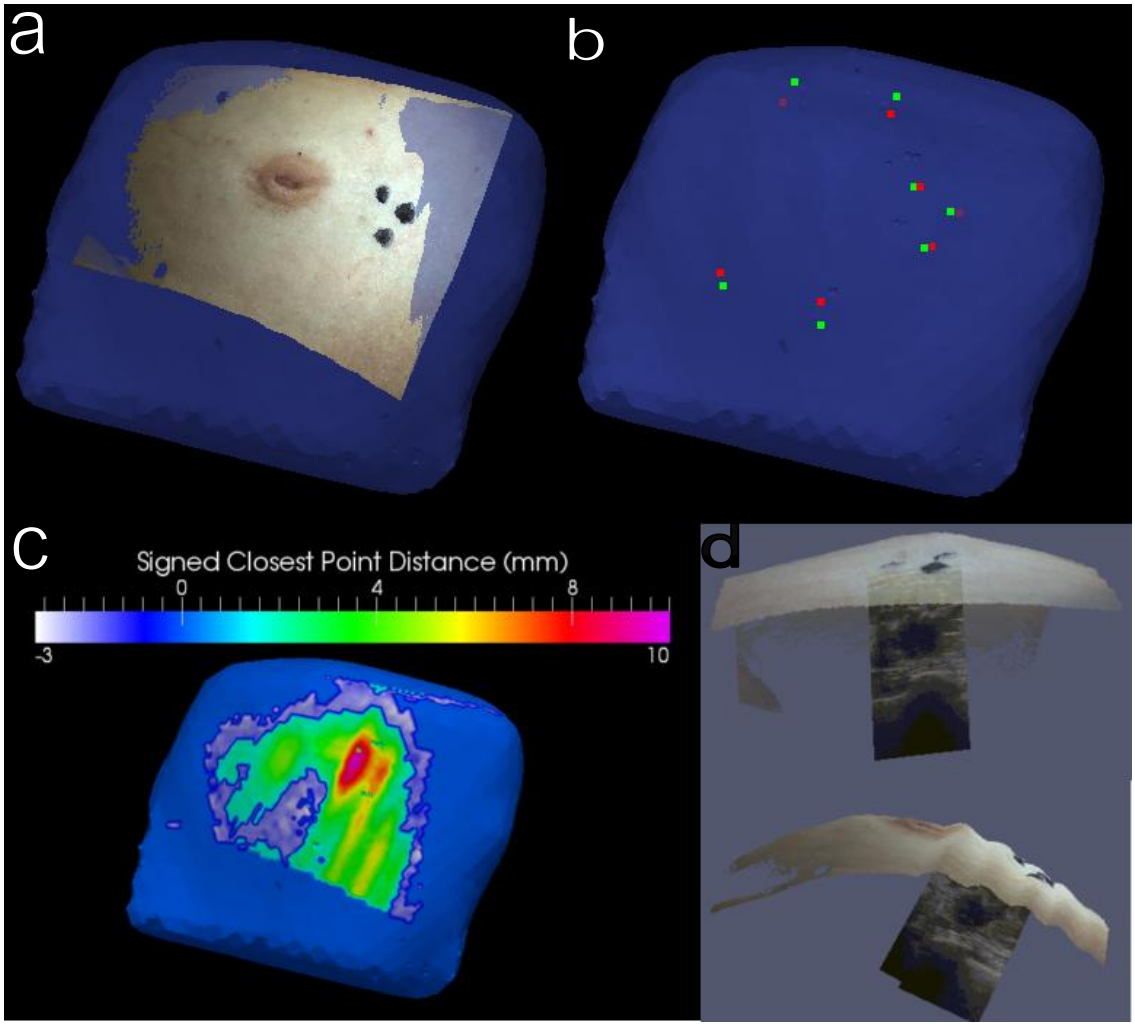

Figure 3: a) Registered digitized breast surface overlaid onto MR generated mesh. b) MR fiducial center points (green) with registered physical space fiducial center points (red) overlaid onto patient specific mesh. c) Signed closest point distance map between laser range scanner point cloud and mesh surface nodes. d) Two orthogonal views of a textured point cloud of the breast with calibrated ultrasound slices showing tumor location in physical space.

The digitized breast surface acquired by the tracked laser range scanner was registered to the patient specific mesh using corresponding landmarks. The digitized breast surface is shown registered to the patient mesh in Figure 3a. The fiducial registration error was 3.4 mm. Figure 3b shows the mesh and MR fiducial center points with the registered physical space fiducial centers. The surface alignment was inspected by calculating the signed closest point distances between the point cloud and mesh surface nodes. The average closest point distance was 1.76+/- 0.502mm. A signed closest point distance map is shown in Figure 3c. Figure 3d shows how tumor location can be viewed in respect to the breast surface by superimposing the LRS point cloud with select ultrasound slices.

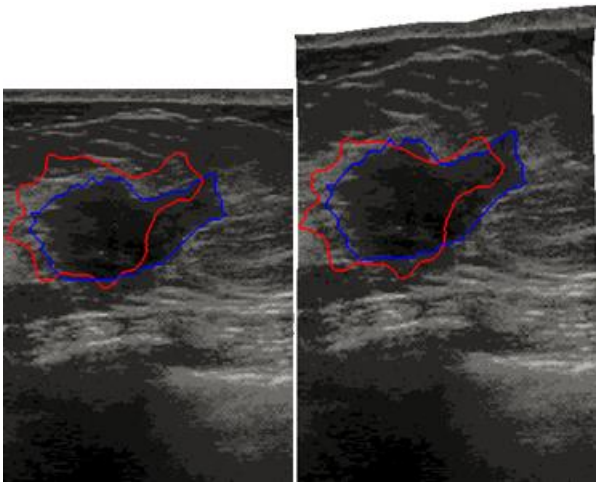

Figure 4: Left: Uncorrected ultrasound slice with uncorrected ultrasound tumor contour (blue) and MR contour (red). Right: corrected ultrasound slice with ultrasound tumor contour (blue) and MR contour (red).

Following registration, the ultrasound slices and their corresponding tumor contours are corrected to compensate for the tissue compression applied by the ultrasound transducer. Figure 4 shows an uncorrected and a corrected ultrasound slice. The blue outline is the ultrasound tumor contour while the red outline is the registered MR tumor contour. The average MHD value for the seven uncorrected US tumor contours was 2.68 +/- 0.6846 mm. The average MHD value for the seven corrected US tumor contours was 2.0814 +/- 0.4454 mm. The average distance from the centroid of the uncorrected US tumor contour and the MR tumor centroid was 3.93 +/- 1.2795 mm, while the centroid distance from the corrected US contours was 3.212 +/- 0.985 mm. Figure 5 shows two plots, one of the MHD values for the corrected and uncorrected tumor contours and the centroid distances for the corrected and uncorrected tumor contours.

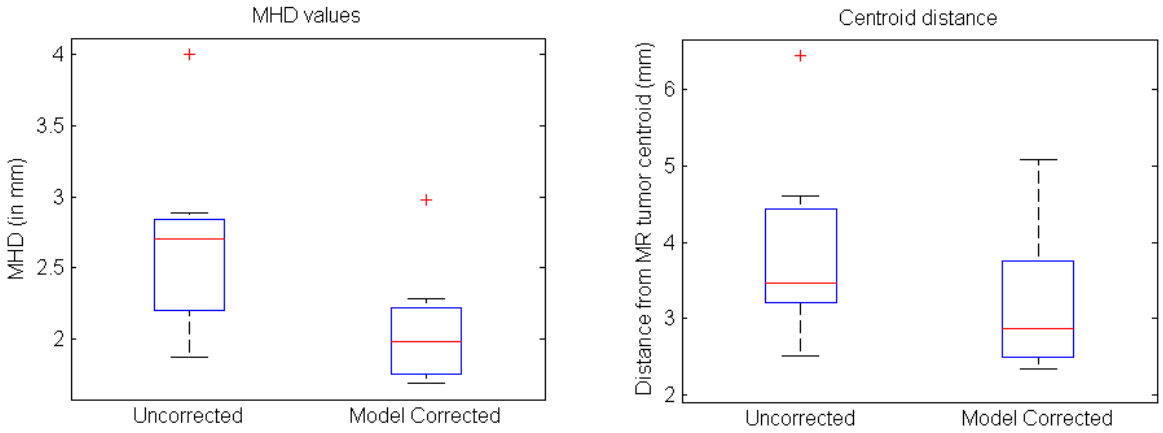

Figure 5: Tumor alignment errors for the corrected and uncorrected ultrasound slices. The modified Hausdorff distance (MHD) between the co-aligned MR tumor contours and the US tumor contours are reported for the uncorrected and model corrected ultrasound slices. The distance between the MR tumor centroid and the US tumor centroids are also reported. The red line inside the box represent the mean and the edge of the boxes represent the 25th and 75th percentiles, and the lines extend to the most extreme observation points not considered as outliers.

In each case, the corrected ultrasound contours yielded a smaller average distance than the uncorrected ultrasound contours. Figure 6 shows three out of the seven slices processed and show the corrected ultrasound slices overlaid onto their corresponding MR slices. The right hand column of Figure 6 shows US (blue) and MR (red) tumor contours as well as the reported MHD value between the two contours.

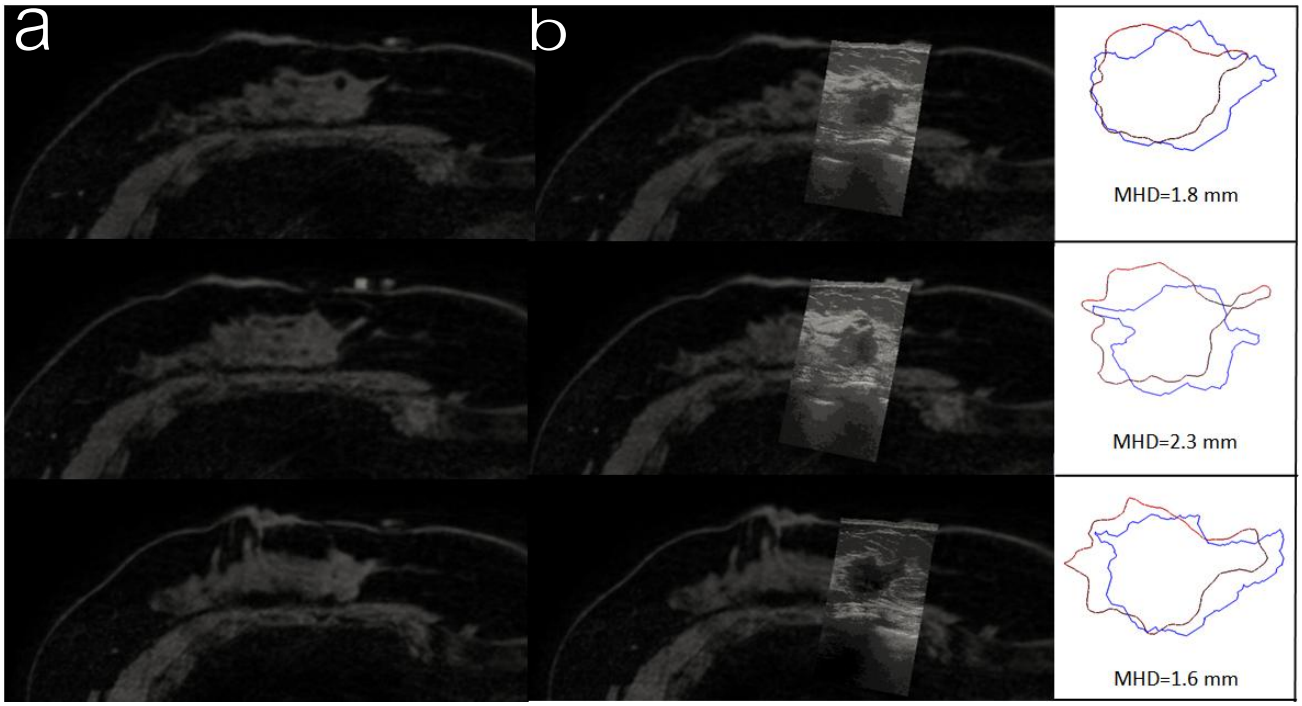

Figure 6: Column (a) is three supine MR slices, Column (b) shows three different registered ultrasound slices overlaid on the corresponding MR slice. The third column shows MR contours (red) and corrected US contours (blue) as well as the MHD values for the two contours.

4. DISCUSSION

The results of the overall surface alignment are on average less than 2 mm. However, multiple inspiration and expiration events happen over the 20-40 seconds that it takes for the laser range scanner to pass across the whole surface of the breast. This causes a rippling effect to be present in the point cloud collected by the LRS. This is evident in the bottom image in Figure 3D. The rippling due to respiratory motion increases a mismatch between the point cloud and mesh surface. This is propagated to the closest point distance map shown in Figure 3c where the largest error (10mm) is at the location of the largest inspiration peak on the point cloud. These respiratory affects can be diminished by using a faster scanner or a different digitization device, such as a stereo vision camera system, where capture of the breast surface occurs at the speed of the camera frame rate (usually <1second).

The model corrected ultrasound slices produced a better average alignment with the MR tumor contours than the uncorrected tumor contours. A Wilcoxon signed rank test was performed to test for differences between the corrected and uncorrected MHD values (significance at p-value < 0.05). There was a significant improvement in tumor alignment when using the model corrected ultrasound slices ($p=0.015$). There was not, however, a significant difference (p-value=0.078) between the corrected and uncorrected tumor centroid distances. Sources of variability that may have contributed to the error is the uncertainty of manual segmentation of the tumor borders in the ultrasound and MR images. Ideally, in the future we will acquire pre and post contrast enhanced magnetic resonance images to get a concrete and user independent tumor border in the MR images. It should also be noted that multiple sources of error may have contributed to the final misalignment of the US and MR tumor contours. Errors associated with the optical tracking equipment, tracked ultrasound calibration, and ability to accurately localize the fiducial center points may be related and

not necessarily additive leading to an uncertainty of how the noises of the system propagate. This uncertainty is characteristic of any realistic guidance platform.

While we are pleased that the surface of the LRS and the surface of the patient mesh were adequately aligned, our real concern is the accuracy of the subsurface features, particularly the cancerous lesion located within the fibro glandular tissue. Figure 6 shows successful alignment between the ultrasound images to the MR slices, with especially promising correspondence between the pectoral muscle and fibro glandular tissue in the MR and US images. The average MHD and centroid distance values of the model corrected ultrasound slices and the MR tumors were around 2-3 mm. A surgical oncologist typically aims to remove 5mm of surrounding healthy tissue, so a 2-3 mm error is acceptable for this surgical domain.

5. CONCLUSIONS

In this work we present a workflow for the acquisition of data, processing of images, creation of patient specific models, and validation for an image based guidance system for the removal of cancerous breast lesions. We collected preoperative images and mock intraoperative data from a breast cancer patient scheduled for a lumpectomy to survey our ability to register and validate our alignment accuracy. With our subsurface alignment errors being on average less than 5 mm, we are encouraged to further investigate the potential of utilizing the combination of supine magnetic resonance images, patient specific biomechanical models, and intraoperative tracked ultrasound as a framework for an image guidance system for breast conservation surgeries.

6. ACKNOWLEDGMENTS

This material is based upon work supported by the National Science Foundation Graduate Research Fellowship. This work is also supported by the Vanderbilt VISE Pilot award program and CTSA award No. UL1TR000445 from the National Center for Advancing Translational Sciences. Its contents are solely the responsibility of the authors and do not necessarily represent official views of the National Center for Advancing Translational Sciences or the National Institutes of Health. We would also like to acknowledge sources that have funded this work in part: NCI 1U01CA142565, NCI 1U01CA174706, and NCI 5R25CA092043.

7. REFERENCES

1. Fisher, B., et al., *Comparison of radical mastectomy with alternative treatments for primary breast cancer: A first report of results from a prospective randomized clinical trial.* Cancer, 1977. **39**(6): p. 2827-2839.
2. Fisher, B., et al., *Eight-Year Results of a Randomized Clinical Trial Comparing Total Mastectomy and Lumpectomy with or without Irradiation in the Treatment of Breast Cancer.* New England Journal of Medicine, 1989. **320**(13): p. 822-828.
3. Fisher, B., et al., *Twenty-Year Follow-up of a Randomized Trial Comparing Total Mastectomy, Lumpectomy, and Lumpectomy plus Irradiation for the Treatment of Invasive Breast Cancer.* New England Journal of Medicine, 2002. **347**(16): p. 1233-1241.
4. McGuire, K., et al., *Are Mastectomies on the Rise? A 13-Year Trend Analysis of the Selection of Mastectomy Versus Breast Conservation Therapy in 5865 Patients.* Annals of Surgical Oncology, 2009. **16**(10): p. 2682-2690.
5. Hwang, E.S., et al., *Survival after lumpectomy and mastectomy for early stage invasive breast cancer.* Cancer. **119**(7): p. 1402-1411.
6. Klimberg, V.S., *Advances in the diagnosis and excision of breast cancer*, in *The American Surgeon*. 2003, Southeastern Surgical Congress: Atlanta. p. 11-4.
7. Pleijhuis, R., et al., *Obtaining Adequate Surgical Margins in Breast-Conserving Therapy for Patients with Early-Stage Breast Cancer: Current Modalities and Future Directions.* Annals of Surgical Oncology, 2009. **16**(10): p. 2717-2730.
8. Metaxas, D., et al., *MR Navigated Breast Surgery: Method and Initial Clinical Experience*, in *Medical Image Computing and Computer-Assisted Intervention " MICCAI 2008*. 2008, Springer Berlin Heidelberg. p. 356-363.

9. Eiben, B., et al. *Biomechanically guided prone-to-supine image registration of breast MRI using an estimated reference state*. in *Biomedical Imaging (ISBI), 2013 IEEE 10th International Symposium on*.
10. Behrenbruch, C., et al., *Prone-Supine Breast MRI Registration for Surgical Visualisation.* Medical Image Understanding and Analysis, 2001.
11. Yang, G.-Z., et al., *A Framework for Image-Guided Breast Surgery*, in *Medical Imaging and Augmented Reality*. 2006, Springer Berlin Heidelberg. p. 203-210.
12. Yushkevich, P.A., et al., *User-guided 3D active contour segmentation of anatomical structures: Significantly improved efficiency and reliability.* NeuroImage, 2006. **31**(3): p. 1116-1128.
13. Kass, M., A. Witkin, and D. Terzopoulos, *Snakes: Active contour models.* International Journal of Computer Vision, 1988. **1**(4): p. 321-331.
14. Lorensen, W.E. and H.E. Cline, *Marching cubes: A high resolution 3D surface construction algorithm.* SIGGRAPH Comput. Graph., 1987. **21**(4): p. 163-169.
15. Sullivan Jr, J.M., G. Charron, and K.D. Paulsen, *A three-dimensional mesh generator for arbitrary multiple material domains.* Finite Elements in Analysis and Design, 1997. **25**(34): p. 219-241.
16. Muratore, D.M. and R.L. Galloway Jr, *Beam calibration without a phantom for creating a 3-D freehand ultrasound system.* Ultrasound in Medicine & Biology, 2001. **27**(11): p. 1557-1566.
17. Sonka, M., J.M. Fitzpatrick, and B.R. Masters, *Handbook of Medical Imaging, Volume 2: Medical image processing and analysis.* Optics & Photonics News, 2002. **13**: p. 449-505.
18. T. S. Pheiffer, R. C. Thompson, D. C. Rucker, A. L. Simpson, and M. I. Miga**,** *Model-based correction of tissue compression for tracked ultrasound in soft tissue image-guided surgery',* Ultrasound in Medicine and Biology, 2014 Vol. TBD, Issue TBD, pp. TBD
19. Dubuisson, M.-P. and A.K. Jain. *A modified Hausdorff distance for object matching*. in *Pattern Recognition, 1994. Vol. 1-Conference A: Computer Vision & Image Processing., Proceedings of the 12th IAPR International Conference on*. 1994: IEEE.